A PSO-based Global MPPT technique for Distributed PV Power Generation

H. Renaudineau, F. Donatantonio, J. Fontchastagner, G. Petrone, G. Spagnuolo, J.-P. Martin, and S. Pierfederici

***Abstract*—Photovoltaic systems are one of the main actors in distributed power generation. Especially in urban contexts, the photovoltaic generators can be subjected to mismatching phenomena, due to the different orientation of the modules with respect to the sun rays or due to shadowing. In these cases, the maximum power point tracking function must be designed carefully. In this paper an architecture including one dc/dc converter for each photovoltaic generator is considered. The converters' output terminals are series-connected to a high voltage dc bus, where also a bi-directional dc/dc converter managing the power from/to a storage device is plugged. The functional constraints deriving from the dc/dc converters' connection, the mismatching phenomena, the MPPT capabilities of the inverter, connected with its input terminals at the dc bus, are taken into account in order to determine the best operating point of the system as a whole. The real time constrained optimization problem is solved by using the particle swarm optimization method, which needs the knowledge of the actual current vs. voltage curve of each photovoltaic generator. The practical impact of this need is also discussed in the paper. The feasibility and the performances of the proposed approach are experimentally validated by using a laboratory prototype.**

***Index Terms*—Distributed Power Generation, Photovoltaic (PV) systems, Maximum Power Point Tracking (MPPT), Particle Swarm Optimization (PSO).**

I. Introduction

The distributed control of Photovoltaic (PV) generators fits with the future structure of the electrical system, made of many small/medium power producers connected to a high voltage dc bus. An inverter collects the power at the dc bus and injects it into the grid. Further flexibility is achieved if, at the dc bus, a bi-directional converter manages the power flux from and to a storage unit, thus allowing to the users to profit from the power they produce even if the grid is not available [1] [2]. Especially in an urban context, the PV sources control must employ a Distributed Maximum Power Point Tracking (DMPPT) architecture [3] [4] which improves the energy production with respect to a centralized MPPT and offers additional features in terms of protection, especially in case of fire, and diagnostics. The advantage ensured by solutions based on the dc/dc distributed MPPT is about the 5% compared to a centralized MPPT, as reported in [5] [6]. One dc/dc converter is dedicated to the MPPT function of each PV source control. It is shown in [7] that it is not possible to identify the best configuration between series and parallel interconnection with regard to constraints, both physical and topological. One of the main advantages of the series connection is that each converter has to bear a fraction of the dc bus voltage at its output and then a high voltage boost ratio is not required [8], and it allows to use simple and efficient converters [7]. On this aspect, an energetic efficiency study of DMPPT applications is given in [9].

Some drawbacks resulting from the series connection of the dc/dc converters' outputs have been investigated in literature. The critical steps in the design of such structures have been discussed in [10]: this process has to take into account the converters' parameters, the PV string sizes and the inverter operating voltage. One of the main conclusions concerns the global optimization of the system behavior: even if high efficiency dc/dc converters are used, the best overall performances of the whole system are greatly dependent on the way it is controlled, and not only on the fact that the PV generators produce the maximum electrical power for the actual environmental conditions.

Many factors affect the system's overall performances, but the occurrence of shadowing phenomena affecting the PV generators, the dc/dc converters allowable conversion ratios and the dc-bus voltage regulation operated by the inverter are the main ones.

As for the first aspect, the usual assumption is that each dc/dc converter controls a single PV module, whose power vs. voltage curve has just one maximum. Instead, if the dc/dc converter is dedicated to a PV panel or a string, the bypass diodes let multiple peaks appear in case of partial shadowing.

As concerns the dc/dc converters' and the inverter operating voltages, in [11] their influence on the DMPPT architectures performances is investigated. It is shown therein that, when mismatching conditions occur, the series connection of the dc/dc converters' outputs exhibits multiple plateaus, as qualitatively shown in Fig.1.

In this case, the inverter's Perturb and Observe (P&O) MPPT algorithm operating at the input terminals thereof is not able to ensure the V_{bus} regulation: it might converge indifferently to any of the plateaus so that the tracking of the global maximum power might not be guaranteed.

H. Renaudineau, J. Fontchastagner, J.-P. Martin and S. Pierfederici are with Université de Lorraine and members of the laboratory of GREEN, 2 avenue de la Foret de Haye, 54516 Vandoeuvre-les-Nancy, FRANCE (e-mail: hugues.renaudineau@univ-lorraine.fr; julien.fontchastagner@univ-lorraine.fr; jean-philippe.martin@univ-lorraine.fr; serge.pierfederici@univ-lorraine.fr).

G. Petrone and G. Spagnuolo are with the Università di Salerno, Department of Electronic and Computer Engineering, Fisciano (SA) ITALY (e-mail: gpetrone@unisa.it; gspagnuolo@unisa.it).

F. Donatantonio is with the Università di Salerno, Department of Industrial Engineering, Fisciano (SA) ITALY (e-mail: fadonatantonio@unisa.it).

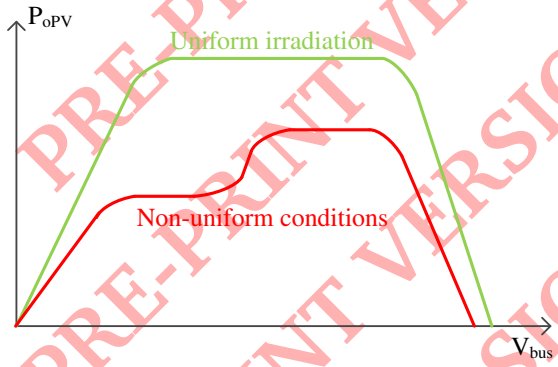

Fig. 1. Power vs. voltage curve of the series connection of the dc/dc converters' outputs.

On the other side, a system working with a fixed and constant bus voltage might definitely lead to a large loss of energy in case of non-uniform conditions. As a consequence, the global optimization problem cannot disregard the voltage V_{bus}. Indeed, in [3] an extensive comparison between DMPPT and centralized MPPT architectures has been carried out by putting into evidence that, if the DMPPT architecture does not interact with the inverter for selecting the best V_{bus} value, the increased energy potentially ensured by the DMPPT solution might be lost.

In conclusion, it is clear that the control of each individual dc/dc converter and the V_{bus} regulation must be performed in a unique optimization algorithm: it must be able to maximize the energy production and to ensure that all the converters fulfill the operating constraints imposed by the DMPPT architecture at the same time.

The centralized control of distributed power electronic circuits dedicated to small PV generators has been recently presented in literature [3]: such a technique allows to achieve both the goals mentioned above. It employs model-based predictive controls in order to keep into account the architecture's functional constraints. Moreover, it is able to achieve the global maximum power point by accounting for the conversion efficiency curve of the dc/dc converters. In [3] a modified P&O MPPT technique allowing to maximize the power injected into the dc bus is described. It is demonstrated that this not always means that the PV units must deliver their maximum available power. In [12] an individual maximization technique based on the extremum-seeking control is combined with a central supervisor acting when the boundaries of the converters' operating conditions are reached. Another solution found in literature consists in adding additional components to deal with non-uniform conditions as in [13] where non-dissipative string current diverters are used to fulfill the converters' operating constraints regardless of the actual environmental conditions. Other centralized DMPPT can be found such as [14] [15] but these techniques, which are based on perturbative algorithms, require a custom definition of the rules depending on the particular optimization problem to be solved.

In this paper a centralized control approach for the DMPPT architecture shown in Fig. 2 is proposed. The real time optimization technique is based on a heuristic algorithm: it maximizes the dc bus power and, at the same time, it keeps into account the possible mismatching affecting the PV sources as well as the functional electrical constraints of the whole circuit. The voltage dc bus requirements are also included in order to ensure that the inverter, which draws the dc power and feeds an ac load or the grid, is able to work properly. In the following, all the aspects included in the optimization process are discussed and formalized in order to be included into the real time code. In particular, in Section II the system is described and its model is derived. Section III is dedicated to the definition of the main equations used by the real time optimization algorithm, thus the objective function and the constraints. In Section IV the strategy used for the periodical acquisition of the voltage vs. current curves of the PV units is described: the main energetic issues and the effect of this operation on the efficiency are discussed. Simulation and experimental results presented in Sections V and VI, respectively, allow to validate the approach proposed in this manuscript.

II. Description of the System under Study

PV applications show discontinuity in the power production. For this reason, PV generators are often hybridized by employing storage devices. In this paper, a system consisting in N PV arrays, each one equipped with a boost converter whose output terminals are connected in series at a high voltage DC bus is considered. A storage unit (e.g. a battery or a bank of supercapacitors) is connected to the same bus by means of a bi-directional boost converter. It is named with a subscript 'a' standing for "auxiliary". In order to focus on the PV power maximization, overcharge or complete discharge of the storage device is not investigated in this paper. The DC voltage bus is supposed to be connected at the input terminals of an inverter. The considered system is represented in Fig. 2 for $N = 3$ as it is used for simulation and experimental validation.

Fig.2 shows the symbols of the electrical variables used in the averaged model given in (1a)-(1f) $\forall k = 1, \ldots, N$:

$$\begin{cases} C_{pv_k}\dfrac{\mathrm{d}V_{pv_k}}{\mathrm{d}t} = i_{pv_k} - i_{L_k} - \dfrac{V_{pv_k}}{R_{p_k}} & \text{(1a)} \\ L_k\dfrac{\mathrm{d}i_{L_k}}{\mathrm{d}t} = V_{pv_k} - r_{s_k} i_{L_k} - (1-d_k)\, V_{o_k} & \text{(1b)} \\ L_a\dfrac{\mathrm{d}i_a}{\mathrm{d}t} = V_a - r_{s_a} i_a - (1-d_a)\, V_{bus} & \text{(1c)} \\ C_{o_k}\dfrac{\mathrm{d}V_{o_k}}{\mathrm{d}t} = (1-d_k)\, i_{L_k} - i_{o_{pv}} & \text{(1d)} \\ \sum_{j=1}^{N} V_{o_j} = V_{bus} & \text{(1e)} \\ i_{inv} = i_{o_{pv}} + i_{o_a} & \text{(1f)} \end{cases}$$

The converters' efficiencies are taken into account by means of the model detailed in the appendix VIII. Indeed, as experimentally confirmed in [16], in some cases, characterized

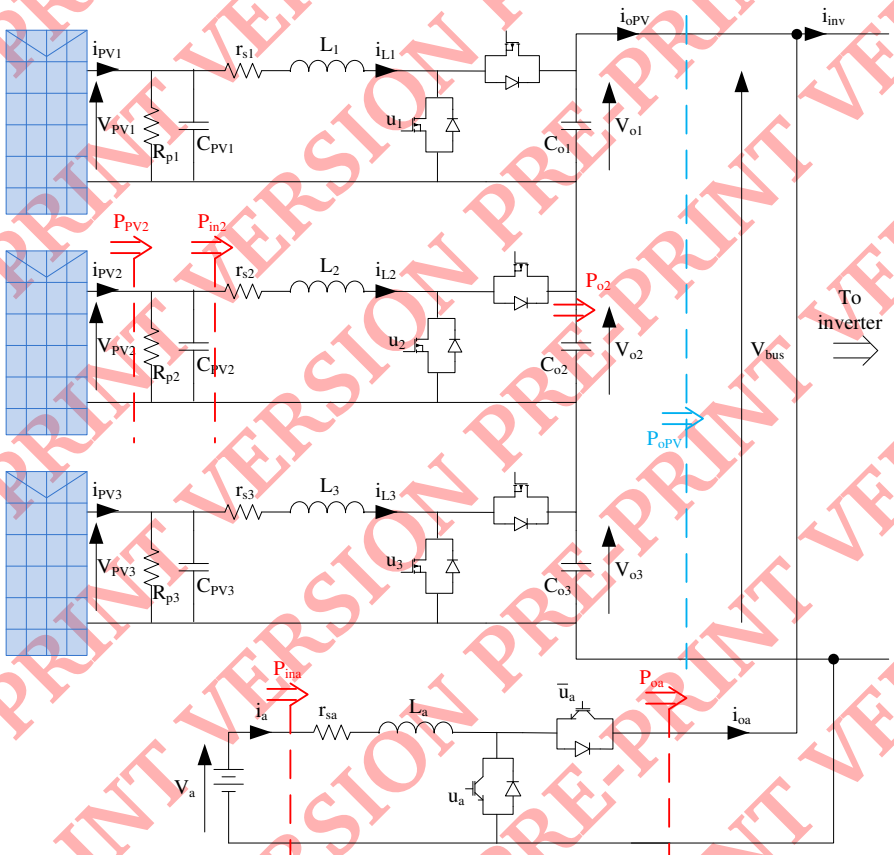

Fig. 2. Scheme of the considered system and notations

by non uniform irradiation values at which the PV sources work, the converters' losses play an important role in the conditions that allow to achieve the maximum power at the dc bus. As shown in appendix VIII, the losses characterizing each converter are modeled through two resistors, r_{s_k} and R_{p_k}. This approach was proposed in [17] and it has been shown to be effective in the optimization of the control strategy for complex systems [18].

A. Control design of the boost converters

The voltage control has been used for the PV voltage setting: a single loop regulation guarantees good dynamic performances and a rejection of the disturbances due to the grid connection, thus ensuring a very precise setting of the voltage at which the PV sources work [19]. The converters' input voltages, that are the PV ones, have been controlled: it would be better to settle their output voltage but, unfortunately, instabilities can arise around the maximum power point in this case [20] [21]. The voltage controller adopted for the boost converters operates on the capacitors' C_{pv_k} charge. The controller design is presented in detail in [16]: it does not depend on the operating point, this feature being very important in PV applications.

The auxiliary converter adopts two control loops: the outer one acts on the energy stored in the bus capacitance, so that the dc bus voltage is indirectly controlled. The inner control loop regulates the power P_a, thus indirectly the current i_a extracted or injected into the storage device. Details about the control technique can be found in [17] and [18].

III. The Constrained Optimization Algorithm

The runtime global and constrained maximization of the power delivered at the dc bus is obtained by means of a Particle Swarm Optimization (PSO) based algorithm. PSO has been shown to be able to improve the MPPT capability under partial shading condition [22] and [23]. Furthermore, it is shown in [24] that the PSO-based MPPT ensure reduced oscillation in steady-state. It has also been already used in PV oriented MPPT problems characterized by a multi-modal power vs. voltage curve of the PV array (e.g. in [25]). PSO-based MPPT has already been applied on parallel structures as in [26], but they have been never applied to any series DMPPT architecture similar to the one presented in this paper and to the objective proposed herein. Still PSO is used in many real time optimization problems in PV applications [27]- [28] confirming the possibility of real time implementation.

A flowchart of the proposed PSO-based MPPT algorithm is given in Fig. 3, where T_{scan} is the time since the last PV curves scan has been realized, T_{min} the minimum time

between two consecutive scan defined in section IV, and the "$restart$" function defined in paragraph III-D.

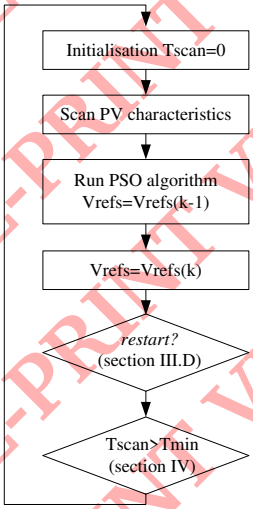

Fig. 3. Flowchart of the proposed PSO-MPPT algorithm

Compared with classical gradient or Newton based optimization techniques, PSO shows rapidity of convergence and ease of implementation, but it has also several additional advantages in the application under study. It does not require any knowledge of the derivative of the objective function, which has not an explicit expression in this case. A finite differentiation aimed at the derivative estimation would be very sensitive to the noise in the practical implementation of the method. Moreover, PSO profits from the fact that it is a global optimization method, so that the risk of remaining trapped into sub-optimal solutions is avoided [29]. Indeed, the PSO does not depends on a starting point. For example, it has also been tested a sequential quadratic programming (SQP) method as programmed through the *fmincon* Matlab function. It has been verified over several configurations that a single start of the SQP algorithm requires approximately the same time. Furthermore, as it is local optimization method, the PSO can fail in searching the global solution unless multi-starts are realized, increasing the convergence time a lot. Finally, the PSO is able to manage inequality constraints by means of penalization functions whose definition is somewhat easy. In Table I are reported the results of the optimization with the PSO compared with the SQP algorithm. The simulated case considers 2 PV arrays irradiated at $1000W/m^2$ while the third only received $100W/m^2$. Under those condition, it can be observed that the SQP algorithm converges to a local maximum, leading to a loss of energy around $239W$ and revealing the superiority of the PSO.

TABLE I
COMPARISON BETWEEN THE PSO AND A SQP ALGORITHM

	PSO	SQP
V_{pv_1}	35.51 V	42.27 V
V_{pv_2}	35.51 V	42.27 V
V_{pv_3}	0 V	11.59 V
V_{bus}	100 V	131.29 V
$P_{o_{PV}}$	404 W	165 W

A. The objective function

The power at the output of the series connected PV generators, namely $P_{o_{PV}}$ in blue in Fig. 2, must be maximized. It is expressed as in (2):

$$P_{o_{PV}} = \sum_{k=1}^{N} V_{pv_k} I_{pv_k} - \hat{r}_{s_k} i_{L_k}^2 - \frac{V_{pv_k}^2}{\hat{R}_{p_k}} \tag{2}$$

In Eq. (2), parameters $\hat{r}_{s_k}$ and $\hat{R}_{p_k}$ are the estimated equivalent losses parameters. Their estimation is detailed in Appendix VIII. Then, the optimization problem is to find the reference vector:

$$V_{refs} = \left(V_{pv_1}^{ref}, \cdots, V_{pv_N}^{ref}, V_{bus}^{ref}\right) \tag{3}$$

that allows to achieve the objective (4):

$$\max_{V_{refs}} \left(P_{o_{PV}} \cdot F_{inv}\right) \tag{4}$$

where F_{inv} is a penalty factor discussed in the subsection that follows.

The PV voltages and currents V_{pv_k} and I_{pv_k} are assumed to be known after the scan of the PV curve, which is run periodically as explained in Section IV. The periodicity of this PV curve sampling is discussed in Sub-section III-D.

B. Constraints

Some constraints are introduced in order to ensure that each dc/dc converter works by fulfilling the ratings of the components it uses. The boost converters must ensure the step-up mode (5a) without violating the components' voltage ratings (5b). The PV arrays must generate electrical power (6a) and the dc bus voltage must fall between assigned lower and upper thresholds related to the inverter operating input voltage range (6b). In (6b), the minimum corresponds to the minimum voltage allowing the controllability of the inverter, while the upper limit is linked to the components' voltage rating as in (5b).

The inequality constraints are:

$$\begin{cases} V_{pv_k} < V_{o_k} & \text{(5a)} \\ V_{o_k} < V_{max} & \text{(5b)} \end{cases}$$

$$\begin{cases} V_{pv_k} \in [0, V_{oc}] & \text{(6a)} \\ V_{bus} \in \left[V_{bus}^{min}, V_{bus}^{max}\right] = \left[V_{bus}^{min}, NV_{max}\right] & \text{(6b)} \end{cases}$$

Thus, the single objective problem has $2N + 1$ non-linear constraints. As studied in [10], from the presence of those constraints the global power maximum can be a not feasible point of the system.

C. The inverter influence

As shown in Fig. 1 and widely discussed in [11], the power vs. voltage curve of the series connected boost converters does not show a number of maximum power points, as a mismatched PV array does, but one or multiple power plateaus where the power keeps theoretically constant in a voltage range. This would lead to an infinite number of optima, that are those ones falling in a whole plateau, thus complicating the optimization procedure performed by the PSO method. The plateaus are exactly flat only theoretically: according to [17], the losses modeled by means of a resistor put in parallel with the converters' output capacitor make the dc bus power slightly decreasing with the bus voltage. According to [30], a small increase in the dc bus power vs. voltage occurs because of the voltage drop of the cables connecting the string to the inverter.

Instead, in this paper, in order to have a unique optimal operating point and avoiding the, purely theoretical, plateaus, the inverter efficiency, which depends on the input voltage at which it works, has been considered. Some papers, e.g. [31], and commercial products data-sheets show that the inverter achieves its maximum efficiency at its nominal input dc voltage, regardless of the input power level. Thus, in the optimization problem, the cost function (2) is multiplied by the following penalization coefficient F_{inv}:

$$F_{inv} = 1 - \alpha_{inv} * (V_{bus} - V_{invOpt})^2 \tag{7}$$

where V_{invOpt} is the dc input voltage at which the inverter shows the maximum efficiency. The coefficient α_{inv} allows to change the convexity of the parabola approximating the inverter efficiency profile. In this paper a small convexity equal to 0.2% has been chosen. Finally, F_{inv} in (4) is the penalty factor accounting for the influence that the V_{bus} value has on the inverter performances.

D. Timing of the PSO-based optimization algorithm

The heuristic control strategy presented in this paper requires the periodical scan of the power vs. voltage curve of each PV array. Such a procedure is described in detail in Section IV. The frequency of this scanning action affects the system power production and the overall system efficiency, so that it must be minimized or a strategy to have an adaptive trigger of this operation must be used. A simple condition to check if the PV curves scan and the optimization process must be launched is based on the measurement of the PV currents i_{pv_k}. A significant change in one of the PV currents is due to a change in the environmental or shadowing conditions, so that the whole control process needs to be launched. An additional condition can be introduced concerning the slope of the PV currents' variations: this would avoid repeated, and useless, optimizations in a short sequence. For the simulations and experimental verification, it is chosen to restart the scan if one of the PV current varies more than 5% of its value. This condition is represented through a "$restart$" function in the flowchart in Fig. 3.

E. Tuning of the PSO parameters

This section gives some considerations allowing to set the parameters of the PSO, especially the number of particles and the maximum number of iterations. More detailed studies of the PSO parameter selection can be found in [32] and [33]. In practice, the PSO performances depends on the irradiation and temperature conditions. For tuning of the parameters, it is chosen to focus on the same case used previously where the SQP fails (Table I), i.e. 2 PV arrays irradiated at $1000W/m^2$ and the third only receiving $100W/m^2$.

At first, the maximum number of iterations is set to a high value (5000) in order to determine the number of particles. In Fig. 4, in function of the number of particles, it is shown the number of times the PSO fails in searching the global optimum out of 1000 optimization runs. It can be observed in Fig. 4 that a number of particles higher than 50 ensures the PSO find the global maximum more than 98% of the cases.

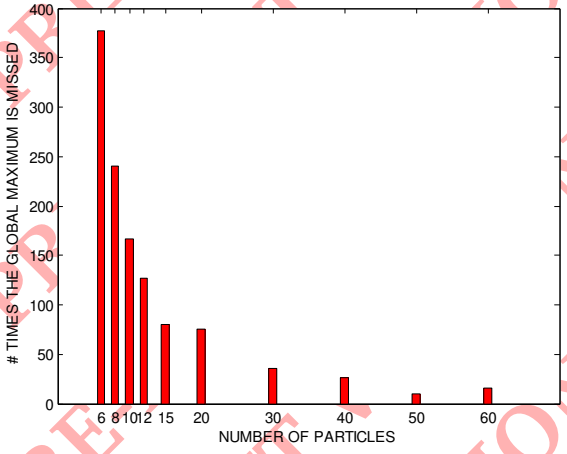

Fig. 4. Accuracy of the PSO function of the number of particles

Also, in Fig. 5 it is shown the calculation time required by the PSO as a function of the number of particles under the same considerations. Even if the calculation time increase with the number of particles, it is verified that this time stays admissible with 50 particles.

With a number a particles set to 50, it is then verified the number of iterations required by the algorithm to converge. In Fig. 6 it is represented the number of iterations required by the PSO to converge for 1000 runs of the optimization. It can be observed in this figure that in more than 98% of the time, the convergence is obtained for a number of iteration between 30 and 90, and that over the 1000 runs it does not exceed 170 iterations. In view of those results, the maximum number of iteration of the PSO algorithm is set to 200.

Then PSO algorithm is executed for a population composed of 50 particles and the maximum number of iteration is set to 200. Those two parameters allows to know the maximum time convergence since the maximum number of calculation is equal to the product of the population size and the number of iterations. Implemented on the dSpace used in experiment, this maximum execution time is around $100ms$.

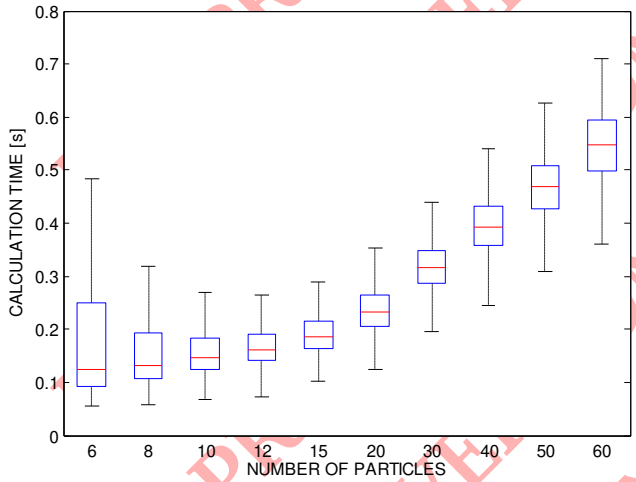

Fig. 5. Calculation time function of the number of particles

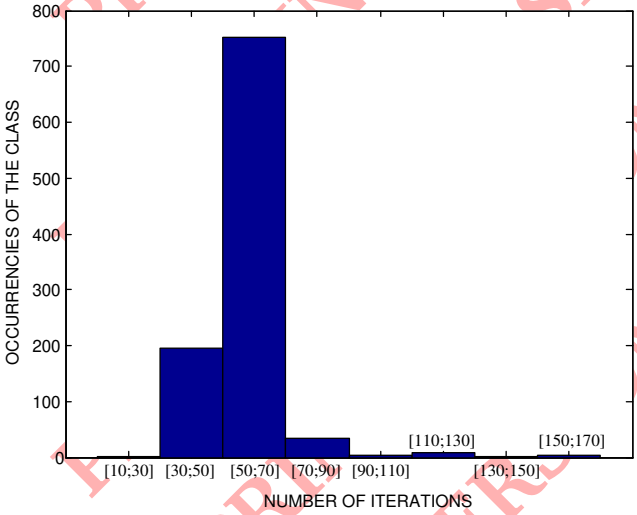

Fig. 6. Number of iteration for convergence of the PSO for 1000 run.

IV. PV CURVES SCAN

The PSO-based global and constrained optimization algorithm assumes that the power vs. voltage curves of the PV units are available before the optimization is run. This aspect must be discussed in detail because of its impact on the system power production.

The system must be perturbed as slightly as possible and for the shortest time interval, so that it is far from the optimal operating point for the shortest possible time interval.

The P-V curve of each PV array is obtained by applying a ramp to the voltage reference of the dc/dc converter that process the power thereof. The ramp slope must be not too high, so that the control is able to properly follow this reference, but the scanning operation must also be fast enough in order to have the smallest impact on the system operation.

The scan has been settled for requiring $4ms$ so that 80 points of the P-V curve are acquired at a sampling frequency of $20kHz$. Before starting the ramp, for $4ms$ a constant low voltage is imposed, by letting the system stabilize on its starting point. It results in a sequence of $8ms$ where the system deliberately does not work at its optimized point, as represented in Fig. 7 for one PV module. Practically, the PV scan of all the PV arrays is done synchronously, thus at the same time, so that the impact on the boost converters' output capacitors' voltages is negligible.

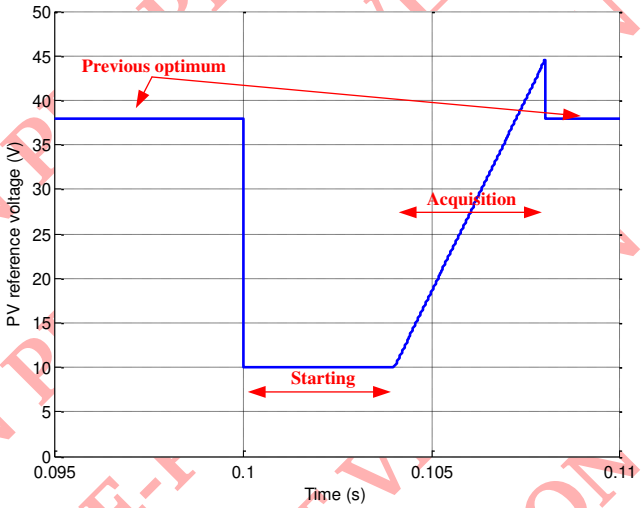

Fig. 7. Reference voltage for the characteristic acquisition

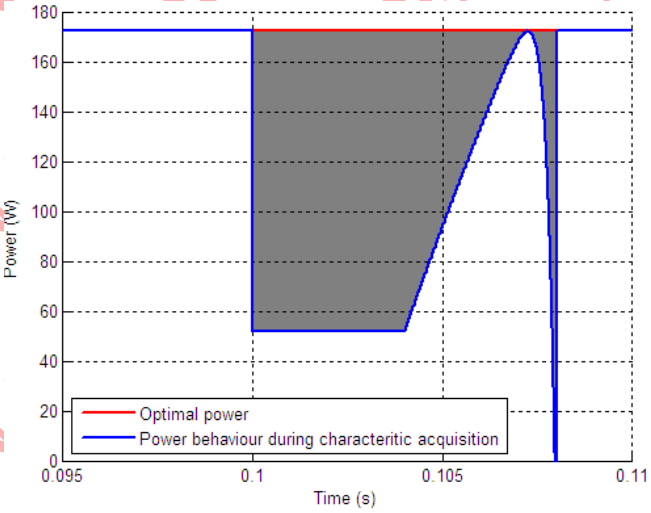

Fig. 8. Energy loss during characteristic acquisition

The value of the PV voltage $V_{pv}\,(t)$ is assumed to be known because it is fixed by the dc/dc converter controller according to the imposed reference. In turn, the PV current is calculated by using the explicit expression employing the Lambert $\mathcal{W}$ function (8) proposed in [34].

By assuming that the PV array exhibits at a given instant a classical static characteristic, the loss of energy due to the curve scan must be compared with an ideal operation in

$$I_{pv} = \frac{V_t}{R_S} \cdot \left[\frac{R_S \cdot (I_{ph} + I_0)}{V_t} - \mathcal{W}\left(\frac{I_0}{V_t} \cdot R_S \cdot e^{\frac{V_{pv}}{V_t}} \cdot e^{\frac{R_S \cdot (I_{ph} + I_0)}{V_t}} \right) \right] - \frac{V_{pv}}{R_{sh}} \quad (8)$$

the MPP at any time. The energy loss is given by (9) and corresponds to the area in grey in Fig.8. If the acquisition procedure is run less than once every $0.4s$, then the loss is negligible ($\leq 1\%$) with respect to the $175W$ that the array is able to deliver by working in the MPP.

$$E_{lost} = 0.695J \quad (9)$$

Finally, it is decided to run the scan process no more than once a second ($T_{min} = 1s$) so that the lost energy stays lower than 0.4%.

Also, the worst case MPPT efficiency can be estimated by referring to the EN50530 standard, which gives the maximum typical rate of change of the irradiance level equal to $100W/m^2/s$. During the $100ms$ needed by the digital controller for running the algorithm in the worst case, the irradiance level would change by almost $10W/m^2$, which is a negligible quantity for medium-high irradiance levels. By assuming a realistic linear relation between the irradiance variation and the power variation, if the system works at an irradiance level close to $1000W/m^2$ the energy losses are 1% of the PV array power. By adding a 0.4% of energy drop due to the PV panel scan it is possible to conclude that the estimation of the "dynamic" MPPT efficiency is 98.6%.

V. Simulation Results

As also stated above, the case of $N = 3$ PV generators, each one controlled by means of a dedicated dc/dc boost converter, has been simulated. Both for the simulation and for the experimental validation, the constraint parameters have been fixed at the following values: $V_{max} = 60V$, $V_{bus}^{min} = 100V$, $V_{bus}^{max} = 180V$ and $V_{invOpt} = 140V$.

At first, a simulation has been run in order to confirm if, according to the procedure described in the Appendix, the estimated values used for the equivalent loss resistors converge to their true value. Fig. 9 confirms this convergence towards the value imposed in the simulated model. The three dc/dc converters have been supposed to be exactly identical each other and a suitable value of their PV voltage reference has been imposed so that the system works in its global optimum in terms of power delivered at the dc bus.

The second simulation concerns the PV curves scan. In order to remove the switching noise, the sampling frequency has been selected equal to the switching one ($f_s = 20kHz$), thus during the acquisition ramp (4 msec), 80 points have been acquired. Moreover, in order to reduce the measurement noise, an averaging process has been used. Figure 10 shows the comparison between the samples acquired during the scan process and the simulated characteristic obtained through (8).

The whole system has been simulated in Saber [35] and the operation of the proposed optimization technique is analyzed under different operating conditions: Fig.11 shows the behavior of the main system variables.

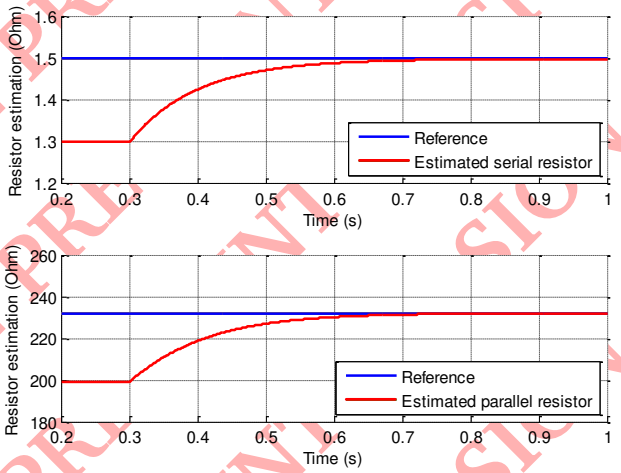

Fig. 9. Verification of the loss estimation - Simulation result

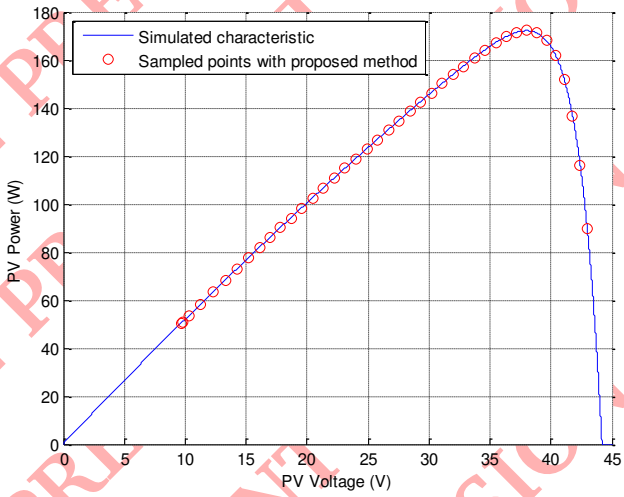

Fig. 10. Verification of the PV characteristic acquisition - Simulation result

At the beginning the three PV units have supposed to receive an irradiation equal to $500W/m^2$. At $t = 0.3s$ the irradiation level at which the third PV array works starts to decrease with a slope of $50W/m^2/s$. At $t = 4.3s$ it keeps a new steady state value of $200W/m^2$, as confirmed by the behavior of the I_{pv3} current in Fig.11.

As stated in Section IV, the PV curves scan is triggered only if the power variation is greater than a fixed threshold. Indeed, because of the constant irradiance conditions after $t = 4.3s$, no more PV curves scans are run after that. In addition, in order to keep the amount of energy loss negligible, it is not run more than once a second. In Fig. 11, the PV scan is put

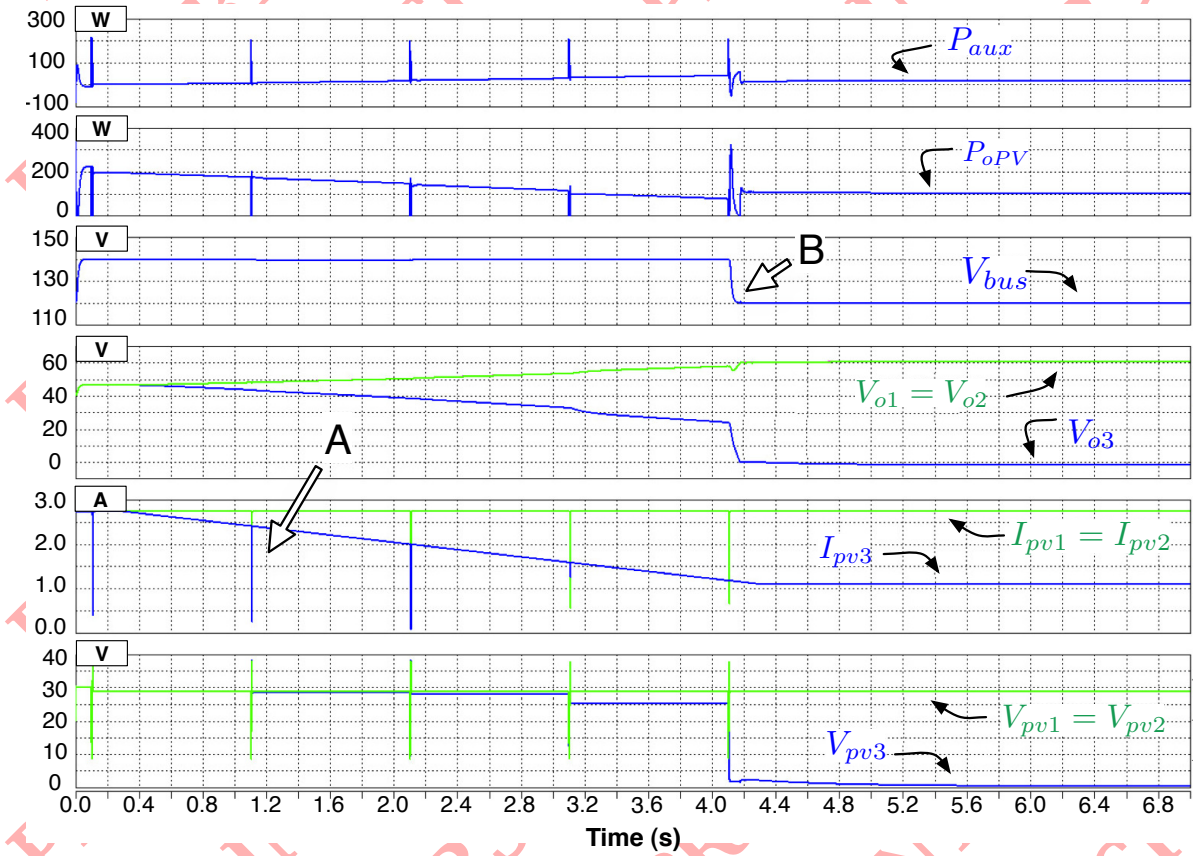

Fig. 11. Simulation of the proposed global MPPT strategy

into evidence by using the letter *A*.

The proposed technique correctly manages the third PV panel when the irradiation it receives falls down. In fact, after $t = 4.1s$, the third dc/dc converter is switched off. At the same time, the global optimization algorithm forces the auxiliary converter to work with a new bus reference voltage (pointed out with a *B* in Fig. 11). The remaining two dc/dc converters are controlled in order to reach the maximum possible output voltage ($60V$), so that all the constraints are fulfilled and the power $P_{o_{PV}}$ is maximized. This optimal behavior would not be ensured by a classical DMPPT solution based on the use of dc/dc converters working independently each other, and it would have not been achieved easily by using a multi-variable P&O MPPT algorithm [3].

Two other simulations have been realized to verify the effectiveness of the proposed approach compared to other possibilities over longer scenarios. In the first simulation, over seven daylight hours, the efficiency of the proposed PSO-based distributed MPPT is compared with the same PV plant connected to a single inverter controlled by a classical P&O MPPT algorithm. The irradiation profile considered in this simulation is shown in the upper plot of Fig. 12. Two of the three PV panels are fully irradiated all along the simulation while the third one is subjected to a partial shadowing between 10:30 and 12:10.

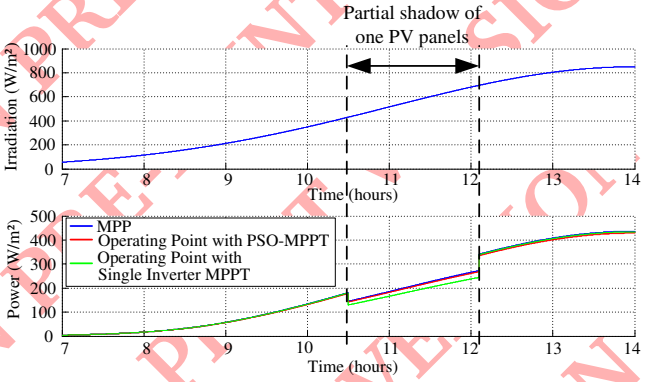

Fig. 12. Comparison of the proposed MPPT with a single inverter controlled with a classical P&O algorithm.

During the occurrence of the partial shadowing, the PV string (consisting of the three PV panels connected in series) power vs. voltage curve exhibits multiple local maxima. For example, at 12:00, the global P-V curve has two distinct maxima as shown in Fig. 13. Under those conditions, the single inverter controlled by a classical P&O MPPT algorithm fails in tracking the global maximum and converges to the local one as can be seen in Fig. 12. The power produced

is in this case limited to around 90% of the possible global maximum.

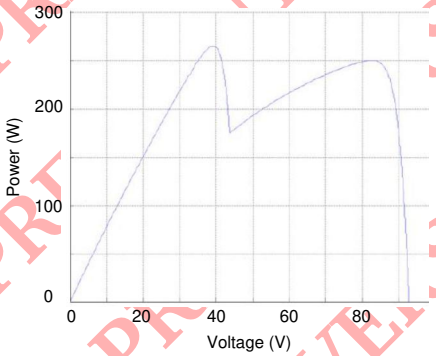

Fig. 13. Static characteristic under partial shading at 12:00.

The power produced in the two cases is depicted in the lower plot shown in Fig. 12. It should be noticed that, for the PSO-MPPT, the time interval dedicated to scanning of the three panels P-V curves does not appear in the figure because of the time scale used (several milliseconds over a few hours), but it is accounted for in the energetic evaluation following here below. For the two MPPT techniques, the total energy produced along this seven daylight hours scenario has been evaluated. It results that the proposed PSO-based distributed MPPT approach shows an energetic efficiency close to 98.1%. In other words, the proposed algorithm ensures that the 98.1% of the maximum available PV energy is produced by the PV generator. This efficiency is calculated at the DC bus and then takes into account the DC-DC boost converters efficiency which do not exist in the single inverter architecture. On the other hand, the P&O MPPT with a single inverter shows an energetic efficiency close to 96.9%. This difference of efficiency is mainly due to a better performance of the proposed distributed MPPT under non-uniform conditions since the global maximum is ensured while the P&O algorithm running on the single inverter converges to the local maximum. This simulation confirms the superiority of the proposed approach if the PV plant is subjected to the partial shadowing during the day, with around 1.2% higher efficiency under the simulated scenario.

A last simulation has been realized considering a more severe shading scenario. In this simulation, every PV panels are mismatch between 10:30 and 12:10 and exhibit multiple power maxima. This time, the proposed distributed PSO-based approach is compared with a classical DMPPT (a similar distributed architecture controlled through a centralized multivariable P&O MPPT). Fig. 14 shows the produced powers under this second scenario. Once again the proposed method shows its advantage. Indeed, the classical DMPPT fails in searching the individual MPP of each panels while the proposed method ensure to work at the global maxima thanks to the scanning process. As done with the last simulation, the difference of efficiency between the two techniques has been quantified on the simulated scenario and the proposed method gives an improvement around 1.5%.

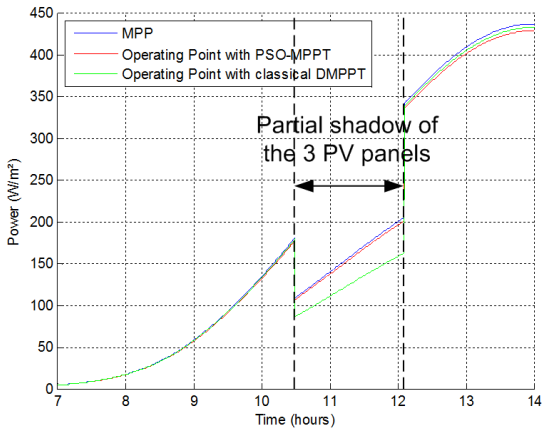

Fig. 14. Comparison of the proposed MPPT with a classical DMPPT.

VI. Experimental validation

The dc/dc converters' controls and the global optimization algorithm have been implemented by means of the dSpace 1103 system. The boost converters have been realized by using Semikron semiconductors, a value of $1mH$ for the boost inductances, $1mF$ for the output capacitances and a value $C_{pv} = 40\mu F$ for the PV dedicated boost converters' input capacitances. In order to perform the test without connecting the prototype to the AC grid, the inverter has been replaced with an electronic load. For this experimental validation the supercapacitors are a Maxwell 48V-165F bank with integrated balancing system. The used PV arrays are single crystal silicon ones with $175W$ maximum power under $1000W/m^2$ and $25°C$.

At first, it has been verified that the calculated losses through estimated resistors fit with the measured losses.
Fig.15 shows the PV voltage, the PV current and the dc/dc converter's output voltage waveforms of one system made of the PV source and the related converter. The two other PV generators are assumed to work in the same conditions, so that the waveforms of the other PV sources are identical. In Fig. 15 the system starts from an operating point resulting from a previous optimization run. Then, the P-V curve is acquired and used for a new run of the optimization algorithm. During the time interval needed by the PSO-based optimization algorithm to compute the new reference signals for the dc/dc converters, the old values of the reference signals are applied just after the P-V curves scan is completed. Once the new references are calculated, they are applied. With the hardware used in this experiment, the optimization algorithm has needed about $30ms$ of calculation time.

The prototype has been also tested in mismatched conditions: Fig. 16 shows the system behavior during the P-V curves scan. The voltage of the partially shadowed panel keeps lower than the other two.

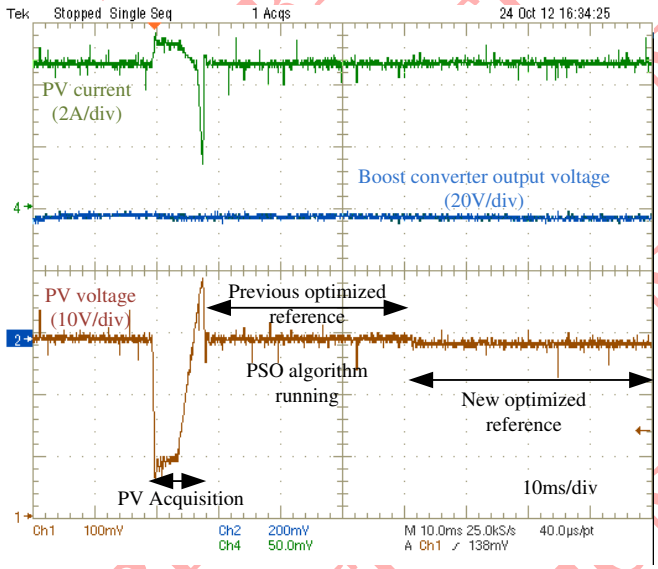

Fig. 15. Experimental verification of the PV characteristic acquisition and optimization process - Evolution of the variables of one of the three PV generators

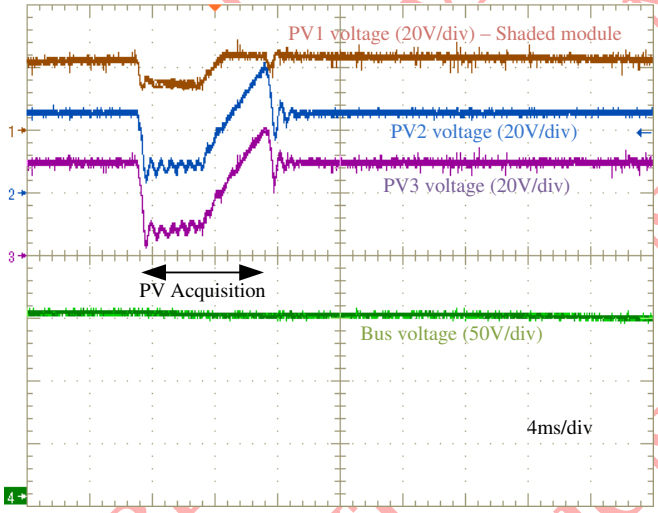

Fig. 16. Experimental verification of the PV characteristic acquisition and optimization process - One panel shaded

VII. Conclusion

In this paper, a global optimization strategy applied to a distributed PV generation system has been proposed. The PV sources are connected to a high voltage bus each one through a dedicated dc/dc converter. At the dc bus a bi-directional dc/dc converter, having at its input a backup unit, feeds or absorbs power.

The optimization of the overall efficiency is performed by using a PSO based algorithm and it needs a periodical acquisition of the power vs. voltage curve of the PV strings feeding the dc/dc converters. This measurement also allows to keep into account partial shadowing conditions affecting the PV sources. The design constraints, including those ones related to the dc/dc converters, the inverter and the PV arrays curves scan have been discussed in the paper.

Simulations and experiments, carried out on a stand-alone system with supercapacitors as auxiliary power supplies, validate the global MPPT method performances.

VIII. Appendix: Losses estimation of the boost converter

This appendix is aimed at describing the technique used to the online estimation of the equivalent losses resistor used in (1a)-(1f). This analysis concerns the PV boost converters loss estimation, because the modeling of the auxiliary converter used to connect the battery to the DC bus is a direct application of the approach given in [17].

Even if the adopted loss modeling employs resistors only, it is worth noting that not only ohmic losses are taken into account. In fact, every loss through the converter, such as core hysteresis and eddy current loss, conduction ohmic losses and switching losses of semiconductors, is taken into account [17]. Particularly, the parallel resistor R_{p_x} does not only represent the capacitor C_x losses through its ESR. Indeed, it is well known the even under null power, boost converters still present losses. This phenomenon is taken into account through R_p while the series resistor is not able to model this behavior. Finally, parameters r_{s_x} and R_{p_x} represent the overall losses through the converter. This is confirmed in Section VI where the calculated losses are shown to fit with the measurement. In [17] the whole analytical study is presented, as well as the load dependency behavior of the model in the case of a single boost converter.

For each PV boost converter, the value of the series resistance is estimated through (10):

$$\frac{\mathrm{d}\hat{r}_{s_k}}{\mathrm{d}t} = \lambda_{s_k} \cdot \left(\hat{P}_{o_k} - P_{o_k}\right) \cdot \left(\frac{V_{pv_k}}{P_{in_k}}\right)^2 \tag{10}$$

where the power P_{o_k} and the estimated power $\hat{P}_{o_k}$ follow (11), and λ_{s_k} convergence coefficient for the estimation. Power P_{in_k} is directly calculated from measurement $P_{in_k} = V_{pv_k} \cdot i_{L_k}$.

$$\begin{cases} P_{o_k} = (1 - d_k) \cdot i_{L_k} \cdot V_{o_k} \\ \hat{P}_{o_k} = P_k - \hat{r}_{s_k} \left(\dfrac{P_k}{V_{PV_k}}\right)^2 \end{cases} \tag{11}$$

As for the estimation of the parallel resistance, in principle it can be done by modifying the estimator proposed in [17] with the same stability validation. However, it has been found that this is not suitable for experiment since this estimation would be directly based on the difference of measured currents i_{L_k} and i_{pv_k}, being far too much sensible to measurement offset precision and noise. Then, it has been chosen to estimate a parallel resistor at the output of the converter exactly as done in [17] according to (12), and then to transfer this resistor at the input before using it.

Parallel resistor is estimated through Eq. (12).

$$\frac{\mathrm{d}\hat{R}_{po_k}}{\mathrm{d}t} = \lambda_{p_k} \cdot \left(\hat{i}_{d_k} - i_{d_k}\right) \cdot \frac{\hat{R}^2_{po_k}}{V_{o_k}} \tag{12}$$

with : estimated current $\hat{i}_{d_k} = (1-d_k)\,i_{L_k}$, $\hat{i}_{d_k} = i_{o_{pv}} + \frac{V_{o_k}}{\hat{R}_{po_k}}$, et λ_{p_k} convergence coefficient associated to R_{po_k}.

This estimated output parallel loss resistor is then brought at the input of the converter considering equal lost power as shown in (13).

$$\frac{V_{o_k}^2}{\hat{R}_{po_k}} = \frac{V_{pv_k}^2}{\hat{R}_{p_k}} \tag{13}$$

Finally, the used estimated parallel loss resistor is deduced from Eq. (14).

$$\hat{R}_{p_k} = \hat{R}_{po_k} \frac{V_{pv_k}^2}{V_{o_k}^2} \tag{14}$$

References

[1] D. Velasco de la Fuente, C. Rodríguez, G. Garcerá, E. Figueres, and R. Gonzalez, "Photovoltaic power system with battery backup with grid-connection and islanded operation capabilities," *IEEE Trans. Ind. Electron.*, vol. 60, no. 4, pp. 1571–1581, 2013.

[2] M. Sechilariu, B. Wang, and F. Locment, "Building integrated photovoltaic system with energy storage and smart grid communication," *IEEE Trans. Ind. Electron.*, vol. 60, no. 4, pp. 1607–1618, 2013.

[3] N. Femia, G. Petrone, G. Spagnuolo, and M. Vitelli, *Power Electronics and Control Techniques for Maximum Energy Harvesting in Photovoltaic Systems*, 1st ed. CRC Press, 2012.

[4] G. Walker and P. Sernia, "Cascaded dc-dc converter connection of photovoltaic modules," *IEEE Trans. Power Electron.*, vol. 19, no. 4, pp. 1130–1139, July 2004.

[5] C. Olalla, C. Deline, and D. Maksimovic, "Performance of mismatched pv systems with submodule integrated converters," *IEEE J. Photovolt.*, vol. 4, no. 1, pp. 396–404, Jan. 2014.

[6] C. Olalla, C. Deline, D. Clement, Y. Levron, M. Rodriguez, and D. Maksimovic, "Performance of power limited differential power processing architectures in mismatched pv systems," *IEEE Trans. Power Electron.*, vol. PP, no. 99, p. 1.

[7] J. Huusari and T. Suntio, "Interfacing constraints of distributed maximum power point tracking converters in photovoltaic applications," in *15th International Power Electronics and Motion Control Conference, EPE-PEMC ECCE Europe*, 2012.

[8] W. Li and X. He, "Review of nonisolated high-step-up dc/dc converters in photovoltaic grid-connected applications," *IEEE Trans. Ind. Electron.*, vol. 58, no. 4, pp. 1239–1250, 2011.

[9] G. Adinolfi, N. Femia, G. Petrone, G. Spagnuolo, and M. Vitelli, "Design of dc-dc converters for dmppt pv applications based on the concept of energetic efficiency," *Journal of Solar Energy Engineering, Transactions of the ASME*, vol. 132, no. 2, pp. 0 210 051–02 100 510, 2010.

[10] N. Femia, G. Lisi, G. Petrone, G. Spagnuolo, and M. Vitelli, "Distributed maximum power point tracking of photovoltaic arrays: Novel approach and system analysis," *IEEE Trans. Ind. Electron.*, vol. 55, no. 7, pp. 2610–2621, July 2008.

[11] R. Alonso, E. Román, A. Sanz, V. Martínez-Santos, and P. Ibanez, "Analysis of inverter-voltage influence on distributed mppt architecture performance," *IEEE Trans. Ind. Electron.*, vol. 59, no. 10, pp. 3900–3907, October 2012.

[12] A. Bratcu, I. Munteanu, S. Bacha, D. Picault, and B. Raison, "Cascaded dc-dc converter photovoltaic systems: Power optimization issues," *IEEE Trans. Ind. Electron.*, vol. 58, no. 2, pp. 403–411, February 2011.

[13] R. Kadri, J.-P. Gaubert, and G. Champenois, "Nondissipative string current diverter for solving the cascaded dc-dc converter connection problem in photovoltaic power generation system," *IEEE Trans. Power Electron.*, vol. 27, no. 3, pp. 1249–1258, March 2012.

[14] F. Boico and L. Brad, "Single sensor mppt algorithm for multiple solar panels configurations," in *IEEE Power Electronics Specialists Conference - PESC*, 2007, pp. 1678–1682.

[15] G. Petrone, C. Ramos-Paja, G. Spagnuolo, and M. Vitelli, "Granular control of photovoltaic arrays by means of a multi-output maximum power point tracking algorithm," *Progress in Photovoltaics: Research and Applications*, vol. 21, no. 5, pp. 918–932, Aug. 2013.

[16] H. Renaudineau, A. Houari, J.-P. Martin, S. Pierfederici, F. Meibody-Tabar, and B. Gerardin, "A new approach in tracking maximum power under partially shaded conditions with consideration of converter losses," *Solar Energy*, vol. 85, pp. 2580–2588, 2011.

[17] A. Shahin, A. Payman, J.-P. Martin, S. Pierfederici, and F. Meibody-Tabar, "Approximate novel loss formulae estimation for optimization of power controller of dc-dc converter," in *IECON - 36th Annual Conference on IEEE Industrial Electronics Society*, 2010.

[18] H. Renaudineau, A. Houari, A. Shahin, J.-P. Martin, S. Pierfederici, F. Meibody-Tabar, and B. Gerardin, "Efficiency optimization through current-sharing for paralleled dc-dc boost converters with parameter estimation," *IEEE Trans. Power Electron.*, vol. 29, no. 2, pp. 759–767, Feb. 2014.

[19] G. Petrone, G. Spagnuolo, and M. Vitelli, "An analog technique for distributed mppt pv applications," *IEEE Trans. Ind. Electron.*, vol. 59, no. 12, pp. 4713–4722, December 2012.

[20] J. Lee, H. Bae, and B. Cho, "Resistive control for a photovoltaic battery charging system using a microcontroller," *IEEE Trans. Ind. Electron.*, vol. 55, no. 7, pp. 2767–2775, July 2008.

[21] C. Rodriguez and G. Amaratunga, "Dynamic stability of grid-connected photovoltaic systems," in *IEEE Power Engineering Society General Meeting*, vol. 2, 2004, pp. 2193–2199.

[22] K. Ishaque and Z. Salam, "A deterministic particle swarm optimization maximum power point tracker for photovoltaic system under partial shading condition," *IEEE Trans. Ind. Electron.*, vol. 60, no. 8, pp. 3195–3206, August 2013.

[23] Y.-H. Liu, S.-C. Huang, J.-W. Huang, and W.-C. Liang, "A particle swarm optimization-based maximum power point tracking algorithm for pv systems operating under partially shaded conditions," *IEEE Trans. Energy Conversion*, vol. 27, no. 4, pp. 1027–1035, Dec. 2012.

[24] K. Ishaque, Z. Salam, M. Amjad, and S. Mekhilef, "An improved particle swarm optimization (pso)-based mppt for pv with reduced steady-state oscillation," *IEEE Trans. Power Electron.*, vol. 27, no. 8, pp. 3627–3638, Aug. 2012.

[25] M. Ngan and C. Tan, "Multiple peaks tracking algorithm using particle swarm optimization incorporated with artificial neural network," *World Academy of Science, Engineering and Technology*, vol. 58, pp. 379–385, 2011.

[26] M. Miyatake, M. Veerachary, F. Toriumi, N. Fujii, and H. Ko, "Maximum power point tracking of multiple photovoltaic arrays - a pso approach," *IEEE Trans. Aerosp. Electron. Syst.*, vol. 47, no. 1, pp. 367–380, Jan. 2011.

[27] M. Alam, F. Khan, and A. Imtiaz, "Optimization of subcell interconnection for multijunction solar cells using switching power converters," *IEEE Trans. Sustain. Energy*, vol. 4, no. 2, pp. 340–349, Apr. 2013.

[28] A. Bidram, A. Davoudi, and R. Balog, "Control and circuit techniques to mitigate partial shading effects in photovoltaic arrays," *IEEE J. Photovolt.*, vol. 2, no. 4, pp. 532–546, Oct. 2012.

[29] R. Poli, J. Kennedy, and T. Blackwell, "Particle swarm optimization - an overview," *Swarm Intell.*, vol. 1, pp. 33–57, 2007.

[30] L. Jiang, W. Zhang, D. Dong, I. Cvetkovic, F. Lee, P. Mattavelli, D. Boroyevich, and P. Kong, "R-based mppt method for smart converter pv system," in *Applied Power Electronics Conference and Exposition (APEC)*, 2012.

[31] D. King, S. Gonzalez, G. G.M., and W. Boyson, "Performance model for grid-connected photovoltaic inverters," Sandia National Laboratories, Tech. Rep., 2007.

[32] Y. Shi and R. Eberhart, "Parameter selection in particle swarm optimization," *Evolutionary Programming VII, Lecture Notes in Computer Science*, vol. 1447, pp. 591–600, 1998.

[33] I. Trelea, "The particle swarm optimization algorithm: convergence analysis and parameter selection," *Information Processing Letters*, vol. 85, pp. 317–325, 2008.

[34] D. Picault, B. Raison, S. Bacha, J. De La Casa, and J. Aguilera, "Forecasting photovoltaic array power production subject to mismatch losses," *Solar Energy*, vol. 84, pp. 1301–1309, 2010.

[35] SABER simulation platform, Synopsys 2013 (http://www.synopsys.com/Systems/Saber/Pages/default.aspx).